

# A NEW THREE AXIS LOW POWER MEMS GYROSCOPE FOR CONSUMER AND INDUSTRIAL APPLICATIONS

A.D. Oliver<sup>1</sup>, Y.L. Teo<sup>2</sup>, A. Geisberger<sup>3</sup>, R.F. Steimle<sup>3</sup>, T. Cassagnes<sup>2</sup>, K. Adhikari<sup>1</sup>, D. Sadler<sup>1</sup>,  
and A. McNeil<sup>1</sup>

<sup>1</sup>Freescale Semiconductor, Tempe, AZ, USA

<sup>2</sup>Freescale Semiconductor, Toulouse, France

<sup>3</sup>Freescale Semiconductor, Austin, TX, USA

## ABSTRACT

The manuscript reports a new commercially available three axis gyroscope, the Freescale<sup>®</sup> FXAS21002C. The 6.8 mW power consumption is 20% less than the nearest competitor's three axis device while meeting standard consumer device parameters. The three axis gyroscope has two proof masses and an open loop control scheme. The open loop architecture and the discontinuous control scheme contribute to this differentiated power consumption.

## KEYWORDS

Gyroscope, 3-axis, low power.

## INTRODUCTION

The device reported here has the lowest power consumption of any three axis gyroscope reported in the literature or on internet datasheets [1-5]. Low power sensors are an important enabler for the "internet of things" especially if the sensors are always on and are also important for wearables or mobile applications. This sensor has two sense masses, a rotating disk for combined X and Y sensitivity, which saves power by combining drive signals, and a tuning fork design for Z axis sensitivity. Table 1 compares this device to other devices reported in the literature or online.

Table 1: 3 axis commercial MEMS gyroscopes

Reference	Published	Power (mW)
Prandi [1]	Y	22
Competitor 1 [2]	N	15
Competitor 2 [3]	N	14
Competitor 3 [4]	N	8.3
Competitor4 [5]	N	12
<b>FXAS21002C</b>	<b>Transducers 15</b>	<b>6.8</b>

All these devices are about 1 mm thick and range from 3 mm x 3 mm to 4 mm x 4 mm in outline. Each has an SPI interface and an I2C interface, with more than one low power mode, and multiple output rotation ranges. The Freescale<sup>®</sup> device, however, has a better temperature coefficient of sensitivity on the Z axis than its competitors at

$\pm 0.01\%/^{\circ}\text{C}$  and equal to or better temperature coefficient of offset at  $\pm 0.01$  dps/ $^{\circ}\text{C}$ .

## SYSTEM DESIGN

This gyroscope has two different drive chains, one for the XY disk and one for the Z tuning fork. The drive chain consists of a capacitance to voltage (C2V) converter to measure the drive mass displacement, an integrator to adjust the phase of the feedback signal and amplification. An automatic gain control (AGC) loop controls the amplification factor and stabilizes the drive mass oscillation. The MEMS output is measured using a sense block, which consists of a capacitance to voltage converter, a demodulator (to remove the drive carrier) and a low pass filter before the 16 bit ADC. The full scale range is selectable by the user from  $\pm 250$  to  $\pm 2000$  degrees per second. The digital output interface is selectable as either I2C or SPI. To reduce power consumption further, it is possible to turn off the ADC in "ready" mode (2.8 mW saved) or the ADC, analog blocks, and MEMS in "standby" mode, only 7  $\mu\text{W}$  total power consumption. A block diagram is shown in Figure 1.

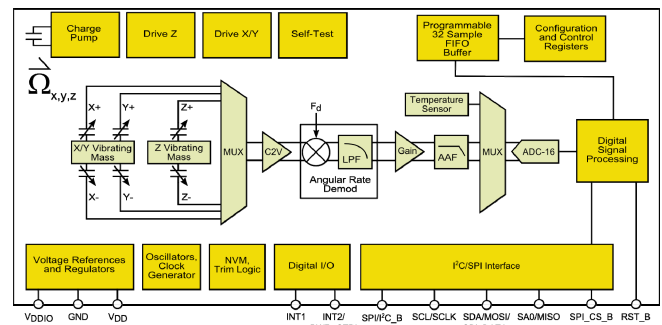


Figure 1: Block diagram of the FXAS21002C integrated MEMS gyroscope.

## ASIC DESIGN

The ASIC for this device is fabricated in a commercial 0.18  $\mu\text{m}$  analog and digital CMOS process with a die size of 2.7 mm x 1.62 mm. Conventional designs for driving the proof mass consists of a charge to voltage convertor, an automatic gain control for the MEMS displacement and an

analog driver. This continuous time control makes the reduction of power consumption difficult. This ASIC used digital circuitry to receive the oscillation information. The drive is only used when oscillation amplification error is greater than the requirement. This reduced the overall power consumed by the drive loop by half with the same rate noise density.

For applications where the power is switched off or into “standby” mode, the startup time of the gyroscope is critical. This device has a transition time from standby to active of 60 ms. The startup time of the gyroscope can be divided into 2 phases. The first phase is to find the resonance frequency of the proof-mass and the second phase is to inject the maximum energy in this frequency. The second phase is related to the technology of the ASIC while the first phase is more design dependent. In this ASIC, a frequency search circuitry is implemented, a series of frequencies is injected into the actuator. When the resonant frequency is found, an electrostatic force at that frequency is used to obtain the target displacement.

## MEMS FABRICATION

The XY and Z transducers for this device are shown in Figure 2 and are constructed out of 25  $\mu\text{m}$  thick structural material. The total size of the MEMS die is 2.9 mm by 2.25 mm. To increase the Q of the transducers, they are bonded in a vacuum with an aluminum-germanium bond.

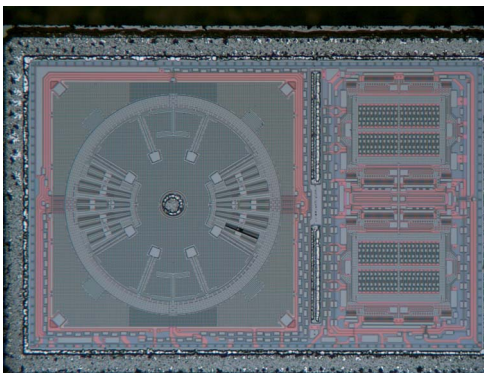


Figure 2: Optical photo of MEMS die showing XY transducer on the left and the Z transducer on the right.

Of the different eutectic material systems, aluminum-germanium bonding was well suited to use in this product because of its material availability and compatibility with existing fabrication processes. Conventional vacuum wafer bonds frequently require a getter. However, because of the excellent vacuum properties of the Freescale<sup>®</sup> process flow, an in situ bake was used in place of a getter resulting in lower process complexity and cost savings.

In order to test whether a getter was necessary to maintain vacuum levels over the lifetime of the product, extended elevated temperature bakes (125 C and 250 C) were performed at wafer level. No systematic decrease in vacuum level was detected. In fact, over time the vacuum

level showed a small increase due to getting of residual gasses presumably by the silicon surfaces in the MEMS device.

## MEMS DESIGN

The architecture of this three axis gyroscope is open loop and requires a high level of vacuum. The cavity vacuum level permits sense Q levels that provide very little phase delays in the sense resonant amplifier. Offset performance benefits from this since any changes in quadrature from package stress or temperature changes do not influence the rate channel. In addition, changes in the cavity pressure across temperature do not need to be compensated. On the drive side, the Q achieved a level sufficient to run the drive on the MEMS devices using a low voltage CMOS technology and with considerable mechanical amplification that makes digital drive signals possible.

## SIMULATION

A unique issue that was seen during development of the three axis gyro is something referred to as abrasion. During the wafer back-grind process vibrations from the grind wheels would excite vertical modes of comb finger cantilever structures. Figure 3 is an overview image of the XY gyroscope transducer indicating structures where such abrasion was found. Figure 4 provides some detailed view of the abrasion locations and the debris generated from the issue.

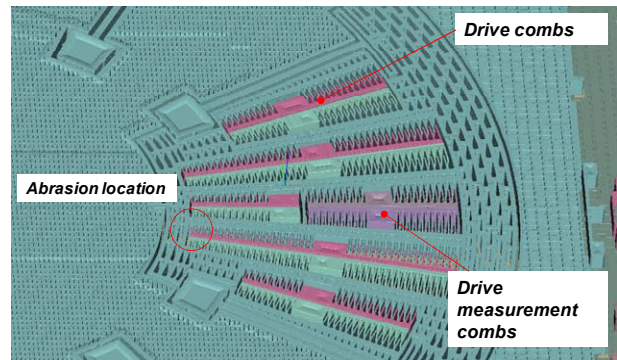


Figure 3: Detailed view of the XY transducer.

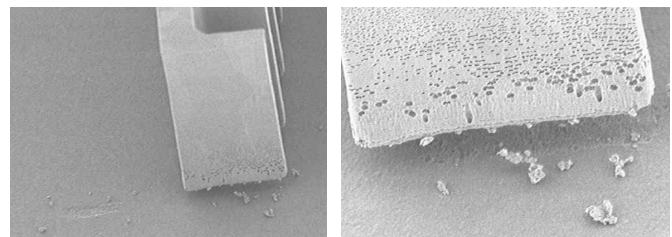


Figure 4: Detailed view damage encountered during development of the gyroscope.

Evidence of abrasion was seen only in the one location denoted. The simple approach to reducing the finger length at the primary issue location only caused the damage to

move to the opposite end of the structure.

The grinding process produces a broad spectrum of acceleration input and the asymmetry of the comb fingers was responsible for injecting energy into the vertical flexing modes of the part. The improved design simply shifted the anchor location to balance the cantilever structure and reduce vibration amplitude at both ends, while not having a detrimental impact on the drive torque produced. The result of the simulation is shown in Figure 5.

Simulations were also crucial in investigating early mechanical failures and how they could be corrected by design. Figure 6 shows the output of a finite element simulation during mechanical shock on the XY transducer.

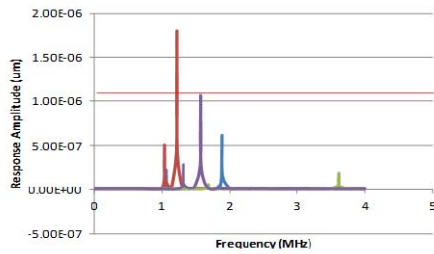


Figure 5: Results from harmonic simulations. The various curves show the various designs that were simulated with the green line showing the final solution. The red horizontal line shows the point where the device would impact the substrate. These simulations matched the experimental data and were used to show that moving the anchor location could address the abrasion issue.

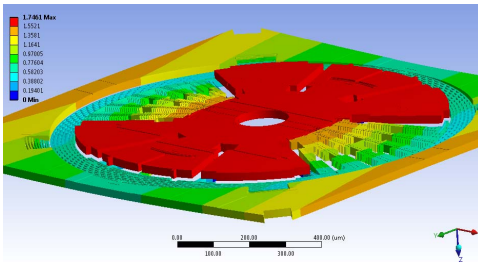


Figure 6: Simulation of the displacement of the XY transducer during mechanical shock.

## ASSEMBLY AND PACKAGING

The gyroscope is packaged in a 4 mm x 4 mm x 1 mm QFN package. The MEMS die, thinned to 500  $\mu\text{m}$ , is die attached to the lead frame paddle and the thinned, 100  $\mu\text{m}$  thick, ASIC die is stacked on top of the MEMS die. Wirebond connections are placed between the MEMS and ASIC and between the chips and the lead frame. Figure 7 is an X-ray image of the assembly and Figure 8, is a photograph of devices on a standard size, 89 mm x 64 mm, playing card.

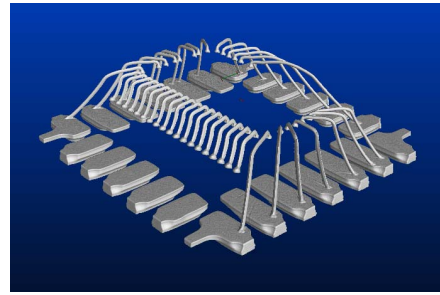


Figure 7: X-ray image of FXAS21002C gyroscope showing the leadframe and the wirebond connections between the MEMS on the bottom and the ASIC that is stacked on top.



Figure 8: FXAS21002C integrated gyroscope shown on 89 mm x 64 mm playing card. The device measures 4 mm x 4 mm x 1 mm.

## EXPERIMENTAL RESULTS

A histogram of power consumption in the active mode is shown in Figure 9. A second histogram in Figure 10 shows the output of the X sensor during X-rotation and a third shows the output of the X sensor during Y rotation. As expected, the transducer shows a large signal on the X sensor during X rotation but almost none during rotation in the Y direction. All histograms used more than 1400 parts with measurements at room temperature. Tests were also conducted at the minimum operating temperature of  $-40^{\circ}\text{C}$  and the maximum operating temperature of  $+85^{\circ}\text{C}$ . In addition to functional tests, devices were subjected to 1.5 m drop tests, 5000 g mechanical shocks, temperature cycling, and temperature and humidity tests. These tests are derived from JEDEC or AEC standards such as JESD22-A113, AEC Q100-008, and JESD22-A103. The stress tests performed during qualification and the parametric tests performed on every part ensure that customers receive high quality products with a low level of defects.

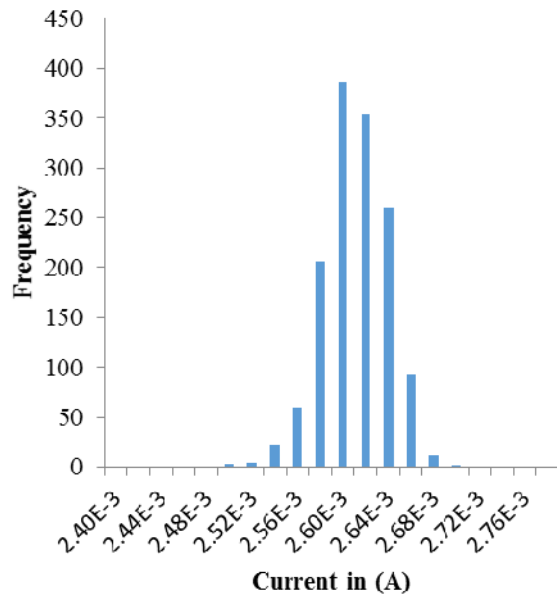


Figure 9: Histogram of current consumption for the FXAS21002C on more than 1400 parts in active mode.

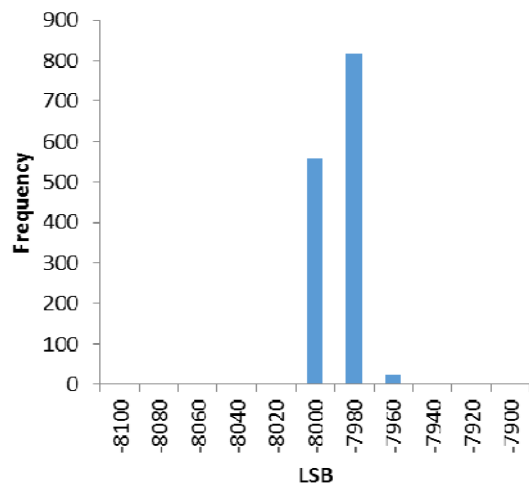


Figure 10: Histogram of more than 1400 parts for the signal from the X transducer during rotation around the X axis.

## SUMMARY

The Freescale FXAS21002C is a production gyro with tens of thousands of parts shipped as of this writing. It has the lowest power consumption of any three axis gyroscope on the market with the same or better performance than its competitors with the same or better performance.

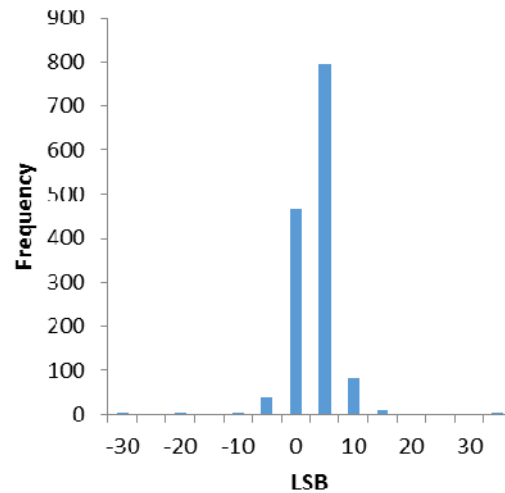


Figure 11: Histogram of more than 1400 parts for the signal from the X transducer during rotation around the Y axis. As expected, the output signal was almost non-existent.

## ACKNOWLEDGEMENTS

The authors gratefully acknowledge the contributions of the ASIC design team in France, the MEMS fabrication team in Texas, USA, the Quality, Validation, Packaging, Product Engineering, and Manufacturing teams in Arizona, USA as well as the ASIC fabrication team, packaging team, and final test team.

## REFERENCES

- [1] L. Prandi, C. Caminada, L. Coronato, G. Cazzaniga, F. Biganzoli, R. Antonello, and R. Oboe, "A Low-Power 3-Axis Digital-Output MEMS Gyroscope with Single Drive and Multiplexed Angular Rate Readout," 2011 ISSCC, pp. 104-106.
- [2] STMicroelectronics, 2014 [Online], Available: <http://www.st.com/st-web-ui/static/active/en/resource/technical/document/datasheet/DM00060659.pdf>. [Accessed 30-Nov-2014].
- [3] Maxim Integrated, 2014 [Online], <http://datasheets.maximintegrated.com/en/ds/MAX21000.pdf>. [Accessed 30-Nov-2014].
- [4] Invensense, 2014 [Online], <http://www.invensense.com/mems/gyro/documents/PS-ITG-3701.pdf>. [Accessed 30-Nov-2014].
- [5] Bosch, 2014 [Online], <http://aebst.resource.bosch.com/media/products/dokumente/bmg160/BST-BMG160-DS000-09.pdf>. [Accessed 30-Nov-2014].

## CONTACT

Andrew Oliver, tel: +1-480-413-3145;  
[Andy.Oliver@Freescale.com](mailto:Andy.Oliver@Freescale.com)